Eddy Covariance Measurements of Turbulent Heat Fluxes over a Grass-Covered Surface in a Tropical Location

ABSTRACT

In this study, an Eddy Covariance (EC) system was deployed to measure the turbulent heat fluxes (sensible and latent heat fluxes) at a farmland located at Obafemi Awolowo University, Ile-Ife, Nigeria. The period of measurement was between 2016 and 2019. The surface of the measurement area was covered by grass (*Axonopus fissifolius*) and changes from leafy-green during the wet season to dry twigs during the dry season. The sensible heat flux, H_s obtained ranged between -0.8 and 181.9 Wm^{-2} while the latent heat flux, H_l varied between 0.9 and 218.0 Wm^{-2}. The maximum daytime value of H_s peaked in January while the maximum daytime value of H_l peaked in October. The sensible heat flux was 59 % higher than the latent heat flux during the Harmattan months (January, February and December), while the latent heat flux was 63 % higher than the sensible heat flux during the wet months (April - November). The study concluded that 91 % of the energy available at the surface during the period of study, was used for evapotranspiration while only 9 % was used for sensible heating as shown by the distribution of the Bowen ratio.

Keywords: Eddy Covariance, Turbulent Heat Fluxes, Sensible Heat Flux, Latent Heat Flux

1. INTRODUCTION

Understanding land-surface-atmosphere processes in different climatic regions are essential for applicable regional climatic projections. Changes in land-surface-atmosphere fluxes such as fluxes of carbon dioxide, water and energy are regarded as

indicators for climate change on regional and global scales due to the ecosystem being influenced by varying environmental conditions [1]. These fluxes influence the evolution of weather phenomena and weather statistics, as the vertical and horizontal structure of the Atmospheric Boundary Layer (ABL) is varying instantaneously to changes in surface fluxes.

The turbulent heat fluxes (sensible and latent heat fluxes) are essential in the exchange of energy between the land surface and atmosphere [2,3]. They control the features and development of the boundary layer, such as the surface temperature, humidity and thermodynamic behaviour [4]. These energy fluxes are also crucial in the general circulation models (GCM), air pollution dispersion and mesoscale air flow [5,6]. A study conducted by Katavoutas et al. [7] pointed out that human comfort is dependent on the surface convective heat fluxes.

The sensible heat flux (H_s) is the energy transfer from the surface to the overlying air. It can also be defined as the vertical temperature gradient of the turbulent transport of heat. That is, it is driven by the difference in the temperature of the earth's surface and the atmosphere [8]. The main mode of transfer of H_s at the surface-air interface is conduction through molecular exchanges. The sensible heat flux is normally directed away from the surface at day time as a result of the surface being warmer than the air above it and vice versa at night time. It determines the mixing strength of the atmosphere, air pollution dispersal and mesoscale air flow. The sensible heat flux (H_S) can be represented as:

$$H_S = \rho c_p K_H \frac{\partial T}{\partial z} \quad (1)$$

where ρ is air density, c_p is the specific heat capacity for constant pressure, K_H is Eddy diffusivity of heat, ∂T is the change in temperature and ∂z is the change in height.

The latent heat flux is the heat flux from the surface to the atmosphere which is associated with evaporation and transpiration of water at the surface and subsequent condensation of water vapor in the atmosphere [8]. It can also be described as the

transfer of energy which occurs as a result of moisture gradient between the surface and the immediate atmosphere. It is driven by the difference in vapour pressure exerted by the water vapour molecules and the immediate air above it. The latent heat flux can be expressed as:

$$H_L = \rho \lambda K_E \frac{\partial q}{\partial z} \quad (2)$$

where ρ is air density, λ is the specific heat of evaporation of water, K_E is Eddy diffusivity of momentum, ∂q is the change in vapour pressure and ∂z is the change in height.

2. THE EDDY COVARIANCE METHOD

The Eddy Covariance (EC) technique is a well-known and defensible approach for the quantification of turbulent exchanges of energy and trace gases between a given ecosystem at the earth's surface and the atmosphere [9]. Using this method, the net transport of the eddy fluxes between the surface and the overlying air is one-dimensional and the vertical flux density is equal to the covariance between the turbulent fluctuations of the vertical wind and the scalar to be transported [10,11]. The EC method became widely used in the early 1990s in the ecological community for the monitoring of water, carbon and energy exchanges in an ecosystem due to its ability to measure in quasi-continuous, long-term manner with minimal disturbance to the ecosystem [12]. Several researchers such as [13,14,15,16,17] have used the EC system to measure fluxes of turbulent heat for the understanding of the ecosystem, testing of land surface models and predicting the responses of the atmosphere to changes in average and severe climate conditions.

The Eddy Covariance (EC) system is the most direct, independent and reliable measurements of sensible and latent energy fluxes [18]. It is comprised of a 3D ultrasonic anemometer for the measurement of u, v, w components of wind speed and an infrared gas analyzer for the measurement of corresponding scalar such as CO_2, H_2O, etc. The instrument is capable of sensing the rapid fluctuations in temperature and wind speed with the largest time resolution [19]. The accuracy of its measurement

technique is dependent on the utilization of correction methods such as tilt correction, spectral correction and application conditions such as steady-state conditions [20]. The most challenging aspect of its methodology is the satisfaction of the requirements of horizontally homogenous surface and steady-state conditions. This method has implemented many turbulent structure assumptions and has also incorporated a lot of correction factors in its measuring techniques which contributes to the accuracy of the turbulent fluxes [21].

The EC method generally considers a fetch-to-height ratio of 100:1 to be adequate [22]. Circulation of the eddy size influencing the vertical transfer of air motion generates a range of frequencies that are essential for the EC system measurements. Therefore, the EC sensors are responsive to high frequencies such as 10 Hz, and the averaging time for the co-variance have low frequencies of the order of 0.01 Hz or less [22]. A 30 minutes or 60 minutes averaging time is frequently used. The key advantage of the EC approach is that there are no assumptions regarding surface properties, such as zero-plane displacement, aerodynamic roughness, or measurement height and no changes are required for atmospheric stability [23].

The method is dependent on numerous assumptions about the surface of interest and the atmospheric conditions during measurements, therefore, appropriate procedure of the instrumentation is required. This will enable minimization of errors and increase the quality of the measurements. Afterwards, a thorough post-field raw data processing and quality control are needed to determine the fluxes from raw measured variables (temperature, wind statistics and gas concentrations). The aim of this research is to study the variability of turbulent heat fluxes as measured by the Eddy Covariance system on a grass-covered surface in Ile-Ife, Nigeria.

3. METHODOLOGY

3.1. The Study Site

The experiment was conducted at the Teaching and Research (T&R) Farm, Obafemi Awolowo University (O.A.U), Ile-Ife (7.53 ^{0}N; 4.54 ^{0}E; altitude 300 m above the sea level, a.s.l), Nigeria as shown in Fig. 1. According to the Koppen-Geiger climate classification [24], the climate is characterised as alternating wet and dry periods between March/April to October and November to February, respectively. The wet season is categorized by recurrent rainstorms due to the high moisture content of the south-westerly airmass. However, during the dry season, there is transport of dry and dusty continental air masses by the north-easterly winds known as Harmattan from the Sahara desert. The Harmattan period usually peaks in January/February. The measurement site is 50 m ×100 m square and covered by grass (*Axonopus fissifolius*) which alters from leafy-green during the wet season to dry twigs during the dry season. The relative humidity in the early mornings is usually about 80% but in the dry season it drops to about 70% or even less. The solar radiation received is always high throughout the year due to the proximity of the location to the equator with maxima values of 1100 and 800 Wm^{-2} at about 13:30 Local Time (LT) in March and August respectively.

The temperatur C, with a mean temperature of about 26.0 ^{0}C. The annual rainfall varies between 1000 mm and 1500 mm with weak surface wind usually less than 2.0 ms^{-1} which is typical of the wind speed distribution in the tropics.

3.2. Instrumentation

An Eddy Covariance (EC) system as shown in Fig. 2, comprising of a 3D ultrasonic anemometer (CSAT3), an open path infrared gas analyzer, (LI-7500) and a temperature-humidity sensor, (HMP60) was used for the measurements of turbulent heat fluxes at the site. The EC system was deployed at the height of 1.81 m above the ground. The system was positioned at the centre of the measurement area such that its fetch was adequate (all sides) to ensure that fetch-height ratio of 100:1 was maintained. This is to ascertain that both the horizontal homogeneity and the steady-state (stationarity) conditions were met. The CSAT3 (Campbell Scientific, Inc.) comprises of a pair of three orthogonal transducers that measures the wind components u, v and w using ultrasonic pulses along the three non-coplanar ray paths, x, y, z. The pair of transducers has a vertical and horizontal measurement paths of 10 cm and 5.8 cm respectively, a path angle of 60^0 from the horizontal direction and a diameter of 0.64 cm each. The CSAT3 was oriented facing the North direction. This was to ensure that the positive horizontal x-axis points to the true North. The anemometer head is integrated with a spirit level bubble to align the sensor in a horizontal plane. The sensor has a cable length of 7.62 m and a weight of 2.8 kg. Its operating temperature ranges between -30 ^oC and +50 ^oC with a voltage supply of 10 -16V DC. It has an electronic box that controls its measurements. The electronics box consists of four military style connectors to prevent the entry of moisture and insects. The connectors are named as RS-232, +12V SDM, Transducer Head and Analog Output. The LI-7500 infrared gas analyser (Campbell Scientific, Inc.) measures the water vapour density and concentration of CO_2 in the atmosphere. The gas analyzer has two sapphire windows that protect the infrared source and detector; and easy cleaning of the sensor. The sensor head has a 12.5 cm open optical path and a 8 mm diameter optical beam. The optical filters which are centred at 3.95 µm provide a reference signal for both the CO_2 and water vapour density. It has a temperature range of -25 ^0C to 50 ^0C. To ensure an uninterrupted power supply, a deep cycle 200VA battery (DC charger) was made available for the system. The period of measurement was between 2016 and 2019.

Fig. 2: An Eddy Covariance System Set-up at the Study Site

3.3. Determination of Turbulent Heat Fluxes

Determination of the turbulent heat fluxes (sensible and latent heat fluxes) using the EC system is centered on the application of Reynolds's postulate, which states that every state variable can be decomposed into their mean and turbulent parts:

$$x = \bar{x} + x' \tag{3}$$

where $\bar{x}$ is the mean variable and x' is the turbulent variable.

The temporal average of the covariance of the vertical wind velocity component (w) and a scalar (x) can be determined by:

$$\overline{w'x'} = \frac{1}{N-1} \sum_{k=0}^{N-1} [(w_k - \overline{w_k})(x_k - \overline{x_k})] \tag{4}$$

The EC system measures the perturbation (turbulent part) of the vertical wind speed and a scalar of interest (temperature or humidity) and then determines the sensible heat flux or the latent heat flux as the covariance of the instantaneous vertical wind and temperature/humidity at a sampling frequency of 10 Hz:

$$\frac{H_s}{\rho c_p} = \overline{w'T'} \tag{5}$$

$$\frac{H_L}{\rho\lambda} = \overline{w'q'} \quad (6)$$

Therefore, the turbulent heat fluxes (sensible heat flux, H_s and latent heat flux, H_L) are equal to the mean air density (**ρ**), multiplied by the covariance between deviations in instantaneous vertical wind speed (w), and temperature/humidity (T or q), and converts it to energy units using the specific heat capacity (c_p):

$$H_s = \rho c_p \overline{w'T'} \quad (7)$$

$$H_L = \rho\lambda\overline{w'q'} \quad (8)$$

3.4. Data Analysis and Assessment

Numerous quality tests were applied to the data, which includes control of steady state flow conditions and intermittent turbulence. A software package called TK2, written by Mauder and Foken [25], was used for quality control and analysis of the Eddy Covariance data. The processes incorporated into TK2 are as follows:

1. Spike detection method based on Højstrup [26] was used to eliminate values that could not be physically removed before the calculation of the variances and covariances.
2. Crosswind correction was performed for the sonic temperature using the procedure of Liu et al. [27].
3. Coordinate transformation was done using the planar fit method of Wilczak et al. [28].
4. The spectral models of Kaimal et al. [29] and Højstrup [26] was used for the spectral corrections.
5. Transformation of buoyancy flux into sensible heat flux was done using the method of Schotanus et al. [30].

6. Corrections for fluctuations in density and mean vertical mass flow of the latent heat flux was done according to Webb et al. [31].
7. Stationarity test was done on the datasets by following the assumptions provided by Foken and Wichura [32]. The values of the measured fluxes were averaged to produce 30 minutes statistics.

4. RESULTS AND DISCUSSIONS

4.1. Mean Meteorological Variables at the Study Location

The monthly average values of mean meteorological parameters observed during the period of study are presented in Table 1. The monthly maximum average values of solar radiation (217 Wm^{-2}) and net radiation (131 Wm^{-2}) were obtained in March. March is a transition month between the dry and wet season. This period is characterised with occasional rain showers which causes washouts and significant reduction in atmospheric turbidity. As a result, there is less attenuation of the incoming radiative fluxes at the surface hence, the high values obtained. The monthly maximum average values of air temperature (29 ^0C), surface temperature (33 ^0C) and soil temperature (31 ^0C) were obtained in February. These values indicate that February experience the hottest weather in the study location. The maximum average value of relative humidity (88 %) was obtained in July and August. This is as a result of the frequent occurrence of precipitation that is prevalent during this period, consequently leading to high atmospheric moisture content.

The maximum average value of wind speed (1.4 ms^{-1}) was recorded in April. This value is attributed to the manifestation of strong wind that is usually accompanied by rainfall. The monthly minimum average values obtained for solar radiation (125 Wm^{-2}), net radiation (83 Wm^{-2}), air temperature (25 ^0C), surface temperature (28 ^0C) and soil temperature (26 ^0C) were recorded in August. August is characterized by the 'short dry period' in the wet season and lasts for about three weeks [33]. This month has the cloudiest weather throughout the year, resulting in low irradiance and consequently, low air, surface and soil temperatures. The monthly minimum average value of relative

humidity (64 %) was recorded in January. This value is attributed to the dry atmospheric condition that is prominent at this period.

The monthly minimum average value of wind speed (0.9 ms^{-1}) at the study location was obtained in the dry season (January, October, November and December). This value indicates that the dry season is a period of tranquil atmospheric condition.

Table 1: Monthly Averages of Mean Meteorological Variables at the Study Location

	Solar Radiation (Wm^{-2})	Net Radiation (Wm^{-2})	Air Temperature (^0C)	Surface Temperature (^0C)	Soil Temperature (^0C)	Relative Humidity (%)	Wind Speed (ms^{-1})
January	179	78	26	30	29	64	0.9
February	185	91	29	33	31	69	1.2
March	217	131	28	32	30	77	1.3
April	207	130	28	31	29	81	1.4
May	201	130	28	30	29	83	1.3
June	180	119	26	29	29	86	1.3
July	147	97	26	28	27	88	1.3
August	125	83	25	28	26	88	1.3
September	161	106	27	28	27	87	1.1
October	188	121	26	29	28	86	0.9
November	195	115	27	31	29	80	0.9
December	185	87	26	31	29	70	0.9

4.2. The Sensible Heat Flux

The diurnal variation of monthly hourly averaged values of sensible heat flux (H_s) from January to December at the study location are presented in Fig. 3. Typically, in the early mornings at about 00:00 to 08:00 Local Time (LT), the values of H_s were low and negative (in the range of -0.8 and -0.1 Wm^{-2}). As the sun rises (at about 08:30 LT), the values of H_s steadily increased to high and positive values (in the range of 4.7 and 181.9 Wm^{-2}). As the sun sets (at about 18:00 LT), H_s steadily decreased again to negative values (in the range of -7.1 and -0.1 Wm^{-2}) till dusk.

The negative values of H_s indicate the decrease in energy at the surface due to the prevailing meteorological conditions (such as solar irradiance) and the surface temperature. As a result, the surface is cooler than the overlying air above it. Conversely, the positive values signify an increase in energy due to intense solar heating at the surface. As a result, the surface is warmer than the overlying atmosphere which leads to a strong mechanical mixing of the boundary layer, hence, high sensible heating.

In January, the daytime maximum value of H_s was 181.9 Wm^{-2}. This is the highest value recorded during the period of this study. This value can be justified by the fact that January is the peak of the dry season at the study location, as such, high solar radiation is received at the surface, hence, high sensible heat flux. As the dry season continued, H_s gradually decreased to 178.5 Wm^{-2} in February and 146.9 Wm^{-2} in March. The wet season commenced in April and the daytime maximum value of H_s observed was 105.7 Wm^{-2}. The maximum value of H_s continued to drop as the wet season progressed to May (85.5 Wm^{-2}), June (75.0 Wm^{-2}), July (69.4 Wm^{-2}) and reached the lowest in August with a value of 56.3 Wm^{-2}.

August has been known to be the cloudiest month throughout the year at the study location [33]. The frequent occurrence of clouds experienced at this period impedes the incoming solar radiation, hence low irradiance. Consequently, the surface is cooler than the overlying atmosphere, hence, low value of H_s. As the transition between the wet and dry season approaches, the daytime maximum value of H_s gradually increased from 86.0

Wm^{-2} in October to 121.4 Wm^{-2} in November and 167.1 Wm^{-2} in December as the dry season re-establishes.

Fig. 3: Diurnal Variation of Monthly Averaged Hourly Values of Sensible Heat Flux

The maximum values of H_s were observed when the solar radiation was at its peak and vice-versa. Therefore, it can be presumed that the solar radiation is the key driver which controls the diurnal pattern of sensible heat flux. That is, it is the solar radiation that cause the temperature change between the surface and the overlying air. A correlation graph between the sensible heat flux and solar radiation was plotted as shown in Fig. 4. The coefficient of determination, R^2 (0.85) obtained from the graph indicate close agreement between the two variables. That is, there is a high degree of association between the two variables.

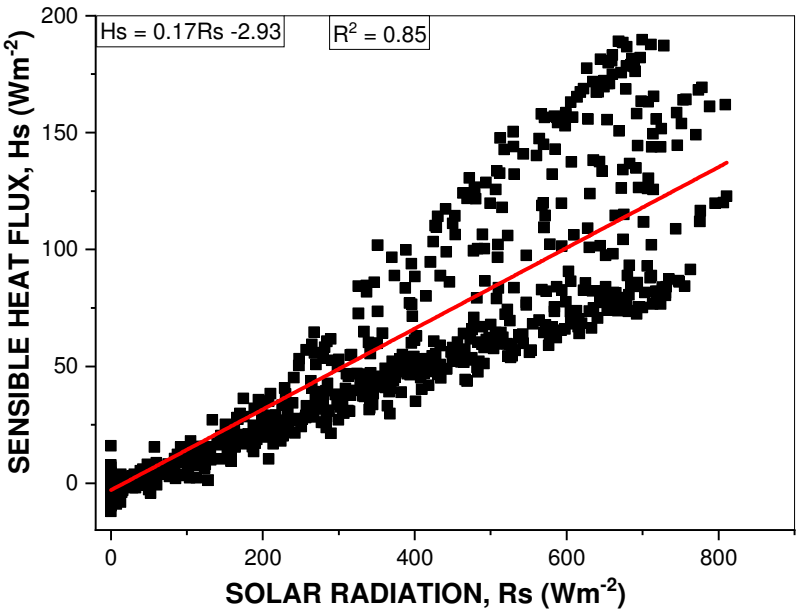

Fig. 4: Correlation between the Sensible Heat Flux and Solar Radiation

4.3. The Latent Heat Flux

The diurnal variation of monthly hourly averaged values of latent heat flux (H_l) from January to December at the study location are presented in Fig. 5. Typically, in the early mornings at about 00:00 to 08:00 Local Time (LT), the values of H_l obtained were low (in the range of 0.3 and 25.0 Wm^{-2}). As the sun rises (at about 08:30 LT), the values of H_l steadily increased (in the range of 27.8 and 218.0 Wm^{-2}). As the sun sets (at about 18:00 LT), H_l gradually decreased (in the range of 0.9 and 62.4 Wm^{-2}) till dusk. The low values obtained during dawn and dusk indicate low rate of evapotranspiration while the high

values obtained in the afternoon signify high evapotranspiration due to high solar radiation that provides heat energy for evaporation.

Fig. 5: Diurnal Variation of Monthly Averaged Hourly Values of Latent Heat Flux

In January, the maximum daytime value of H_l recorded was 69.1 Wm^{-2} and gradually increased to 84.2 Wm^{-2} in February and 153.0 Wm^{-2} in March. As the wet season commenced in April, the maximum daytime value of H_l increased to 172.4 Wm^{-2}, 186.4 Wm^{-2} in May and 190.7 Wm^{-2} in June. The increase in the value of H_l in the wet season can be linked to the high amount of water present at the surface due to high precipitation during the period. The daytime value of H_l dropped to 164.8 Wm^{-2} in July and 133.9 Wm^{-2} in August. The drop in the values of H_l in July and August is as a result of the cloudy conditions experienced in these months. As a result, there is less heat energy to evaporate water from the surface. As the cloudy condition gradually fades away, the maximum daytime value of H_l increased to 175.2 Wm^{-2} in September and 218.0 Wm^{-2} in October. The value obtained in October is the highest value of H_l obtained during the period of study. H_l steadily decreased to 198.0 Wm^{-2} in November and drastically decreased to 136.5 Wm^{-2} in December due to low water content at the surface as a result of dry atmospheric condition which is prominent during this period.

Fig. 6 depicts the diurnal variation of monthly averaged values of both the sensible heat and latent heat fluxes. The sensible heat flux was 59 % higher than the latent heat flux during the Harmattan (January, February and December). This was as a result of the dryness of the surface during this period that is, there was little or no water at the surface. As such, the available energy was being used to warm the surface. In March, the sensible heat flux was relatively of the same magnitude with the latent heat flux signifying equal partitioning of energy between the two fluxes. From April to November, the latent heat flux was 63 % higher than the sensible heat flux indicating that most of the available energy at the surface was used for latent heating.

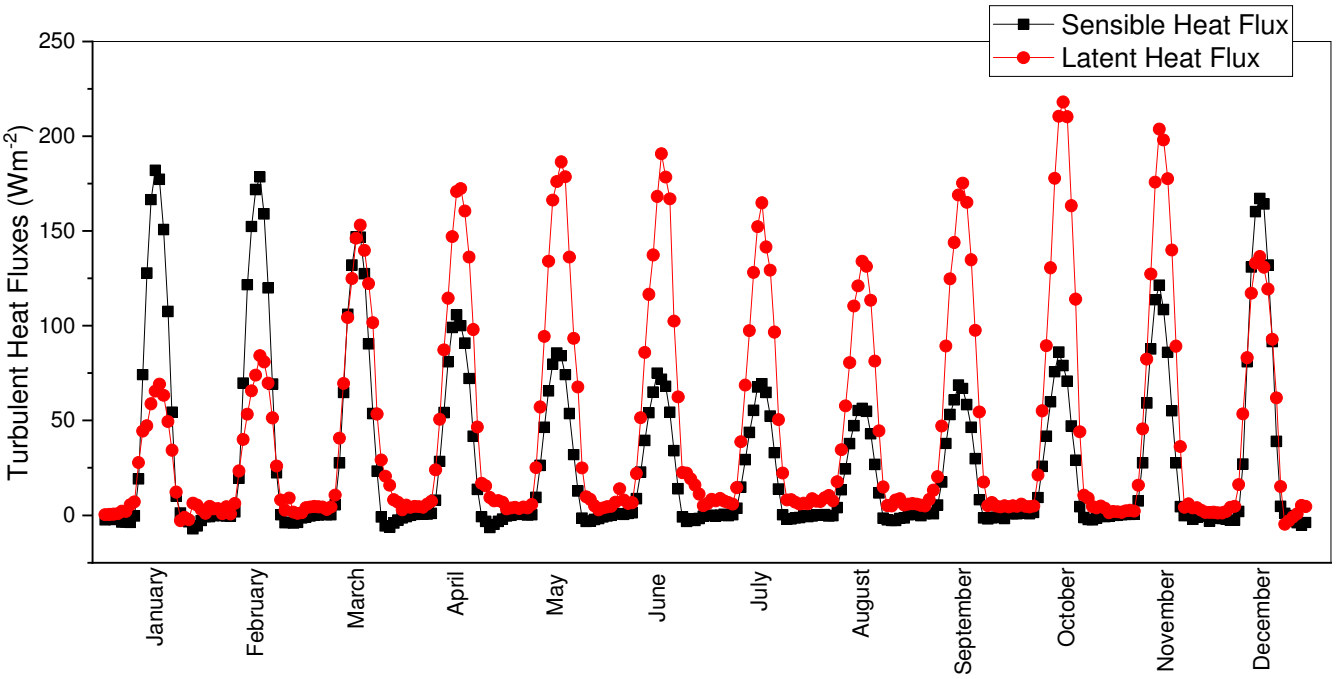

Fig. 6: Diurnal Variation of Monthly Averaged Values of Sensible and Latent Heat Fluxes

Fig. 7 shows the distribution of the Bowen ratio (H_s/H_l), Bo obtained during the period of study. 91 % of Bo was less than 1 (Bo < 1) while 9 % of Bo was greater than 1 (Bo > 1). This can be explained that during the period of study, 91 % of the heat energy at the surface was used for evapotranspiration while only 9 % was used to warm the surface. The high value of Bo < 1 obtained, is a result of the type of surface used in the study which was a grass-covered surface. Therefore, there was minimal radiative heating due to the presence of grass which consequently led to low sensible heating hence, high evapotranspiration.

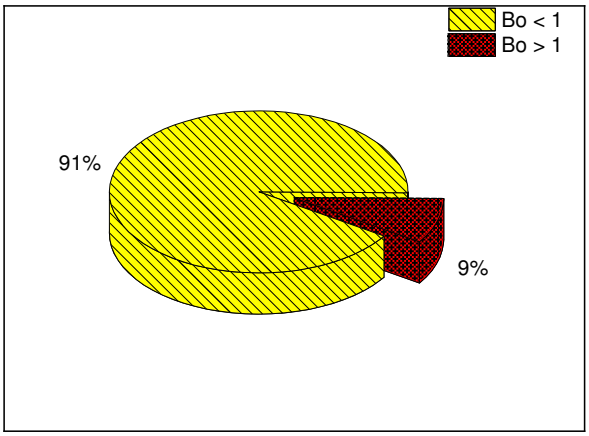

Fig. 7: Distribution of Bowen Ratio, Bo during the Period of Study

5. SUMMARY AND CONCLUSION

This study used the Eddy Covariance System to measure the turbulent heat fluxes (sensible and latent heat fluxes) over a grass covered surface at a Tropical location, Ile-Ife, Nigeria. The period of measurement was between 2016 and 2019. The sensible heat flux ranged between -0.8 and 181.9 Wm^{-2} while the latent heat flux varied between 0.9 and 218.0 Wm^{-2}. The maximum daytime value of the sensible heat flux peaked in January with a value of 181.9 Wm^{-2} while the peak maximum daytime value of the latent heat flux (218.0 Wm^{-2}) was obtained in October. The lowest maximum daytime value of sensible heat flux (56.3 Wm^{-2}) was obtained in August while the lowest maximum daytime value of latent heat flux (69.1 Wm^{-2}) was recorded in January. January is the peak of the dry season, hence, high solar irradiance received at the surface, which lead to high sensible heating and low evapotranspiration due to low surface moisture.

During the Harmattan months (January, February and December), the sensible heat flux was 59 % higher than the latent heat flux while the latent heat flux was 63 % higher than the sensible heat flux during the wet months (April - November). The distribution of the Bowen ratio, Bo shows that 91 % of Bo was less than 1 ($Bo < 1$) while 9 % of Bo was greater than 1 ($Bo > 1$).

The study concludes that during the period of study, the heat energy received at the surface (grass-covered) was majorly used for evapotranspiration while only 9 % was used for sensible heating.

ACKNOWLEDGEMENT

The authors appreciate the support of the members of the Atmospheric Physics Research Group (APRG) at the Department of Physics and Engineering Physics of Obafemi Awolowo University, Ile-Ife, Nigeria during the field experiment.

COMPETING INTERESTS

Authors have declared no competing interests exist.

REFERENCES

1. Schmidt A, Hanson C, Kathilankal J, Law BE. Classification and assessment of turbulent fluxes above ecosystems in North-America with self-organizing feature map networks. Agric For Meteorol. 2011;151:508–520

2. Gentine P, Entekhabi D and Heusinkveld B. Systematic errors in ground heat flux estimation and their correction. Water Resour. Res. 2012;48:W09541, doi:10.1029/2010WR010203

3. Xu T, Bateni SM, Liang S, Entekhabi D and Mao K. Estimation of surface turbulent heat fluxes via variational assimilation of sequences of land surface temperatures from Geostationary Operational Environmental Satellites. J. Geophys. Res. Atmos. 2014;119:780–798.

4. Beringer J and Tapper N. Surface energy exchanges and interactions with thunderstorms during the Maritime Continent Thunderstorm Experiment (MCTEX). J. Geophys. Res.2002;107:4552–4564.

5. Chen F and Dudhia J. Coupling an advanced land -surface/hydrology model with the PennState-NCAR MM5 modeling system, Part I - Model implementation and sensitivity. Weather Rev. 2001;129:569–582.

6. Sridhar V, Elliott RL, Chen F and Brotzge JA. Validation of the NOAH-OSU land surface model using surface flux measurements in Oklahoma. J. Geophys. Res. 2002;107,4418.

7. Katavoutas G, Flocas H and Tsitsomitsiou. Thermal comfort in hot outdoor environment under unsteady conditions. Advances in Meteorology, Climate and Atmospheric Physics, Greece. 2014; 2:195-200.

8. Arya SP. Introduction to Micrometeorology. Academic Press, San Diego, 2001.

9. Sabbatini S, Mammarella I, Arriga N, Fratini G, Graf A, Hörtnagl L, et al. Eddy covariance raw data processing for CO2and energy fluxes calculation at ICOS ecosystem stations. Int. Agrophys. 2018; 32: 495-515. doi: 10.1515/intag-2017-0043.

10. Aubinet M, Vesala T, Papale D. Eddy Covariance - A Practical Guide to Measurement and Data Analysis. Springer, Dordrecht. 2012. doi: 10.1007/978-94-007-2351-1

11. Mauder M, Foken T, Clement R, Elbers JA, Eugster W, Grünwald T, Heusinkveld B and Kolle O. Quality control of CarboEurope flux data-Part 2: Inter-comparison of eddy-covariance software. Biogeosciences. 2008;5:451-462. doi:10.5194/bg-5-451-2008.

12. Chen X, Yu Y, Chen J, Zhang T and Li Z. Seasonal and interannual variation of radiation and energy fluxes over a rain-fed cropland in the semi-arid area of

Loess Plateau, northwestern China. Atmospheric Research. 2016;240–253. http://dx.doi.org/10.1016/j.atmosres.2016.03.003

13. Baldocchi D. Measuring fluxes of trace gases and energy between ecosystems and the atmosphere–the state and future of the eddy covariance method. Global Change Biology. 2014;20:3600-3609. doi: 10.1111/gcb.12649.

14. Järvi L, Rannik U, Kokkonen T, Kurppa M, Karppinen A, Kouznetsov R, et al. Uncertainty of eddy covariance flux measurements over an urban area based on two towers. Atmos. Meas. Tech. 2018;11: 5421-5438. https://doi.org/10.5194/amt-11-5421-2018.

15. Gua L, Massman W, Leuning R, Pallardy S, Meyerse T, Hanson P. The fundamental equation of eddy covariance and its application in flux measurements. Agricultural and Forest Meteorology. 2012;152:135-148. doi:10.1016/j.agrformet.2011.09.014.

16. Kuricheva O, Avilov V, Dinh D, Sandlersky R, Kuznetsov A, Kurbatova J. Seasonality of energy and water fluxes in a tropical moist forest in Vietnam. Agricultural and Forest Meteorology. 2021; 298-299. https://doi.org/10.1016/j.agrformet.2020.108268.

17. Rosa R and Tanny J. Surface renewal and eddy covariance measurements of sensible and latent heat fluxes of cotton during two growing seasons. Biosystems engineering.2015;136:149-161. http://dx.doi.org/10.1016/j.biosystemseng.2015.05.012.

18. Gao Z and Bian L. Measurements of turbulent transfer in the near-surface layer over a rice paddy in China. J. Geophys. Res. Atmos. 2003; 65:112-120.

19. Wang J and Bras R. A new method for estimation of sensible heat flux from air temperature. Water Resources Research. 2008;34: 2281-2288.

20. Foken T, Gockede M, Mauder M, Mahrt L, Amiro BD and Munger J W. Post-field data quality control: Handbook of Micrometeorology: A guide for surface flux measurement and analysis. 2004;181–208.

21. Odhiambo G and Savage M. Sensible heat flux by surface layer scintillometry and eddy covariance over a mixed grassland community as affected by Bowen ratio and MOST formulations for unstable conditions. American Meteorological Society. 2009. DOI:10.1175/2008JHM1008.1.

22. Kaimal J and Finnigan J. Atmospheric Boundary Layer Flows. Ed. Oxford Univ. Press. 1994.

23. Pryor S, Gallagher M and Sievering H. A Review of Measurement and Modelling results of particle atmosphere - surface exchange. Tellus. 2008;60:42-75.

24. McKnight TL and Hess D. Climate zones and types: dry climates (Zone B), in: Physical geography: a landscape appreciation. Prentice Hall, Upper Saddle River. 2000; 212–219.

25. Mauder M and Foken T. Impact of post-field data processing and body variance flux estimates and energy balance closure. Meteorologische Zeitschrift. 2006;15(6):597–609. https://doi.org/10.1127/0941-2948/2006/0167.

26. Højstrup J. A statistical data screening procedure. Measurement Science and Technology. 1993;4(2):153–157. https://doi.org/10.1088/0957-0233/4/2/003.

27. Liu HP, Randerson JT, Lindfors J and Chapin FS III (2005). Changes in the surface energy budget after fire in boreal ecosystems of interior Alaska: An annual perspective. Journal of Geophysical Research. 2005; 110. https://doi.org/10.1029/2004JD005158.

28. Wilczak JM, Oncley SP and Stage SA. Sonic anemometer tilt correction algorithms. Boundary-Layer Meteorology. 2001; 99(1): 127-150. https://doi.org/10.1023/A:1018966204465.

29. Kaimal JC, Wynguard JC, Izumi T and Coto OR. Special characteristics of surface layer turbulence. Quarterly Journal of the Royal Meteorological Society. 1972;98(417):563–589. https://doi.org/10.1002/qj.49709841707.

30. Schotanus P, Nieuwstadt FTM and DeBruin HAR. Temperature measurement with a sonic anemometer and its application to heat and moisture fluctuations. Boundary-Layer Meteorology. 1983; 26(1):81–93. https://doi.org/10.1007/BF00164332.

31. Webb EK, Pearman GI and Leuning R. Correction of the flux measurements for density effects due to heat and water vapour transfer. Quarterly Journal of the Royal Meteorological Society. 1980;106:85–100.

32. Foken T and Wichura B. Tools for quality assessment of surface-based flux measurements. Agric. For. Meteorol. 1996;78: 83 - 105.

33. Obisesan OE. Estimation of Atmospheric Turbidity Parameters in Ile-Ife, Nigeria. Physical Science International Journal. 2021;25(7): 30-40. DOI: 10.9734/PSIJ/2021/v25i730270.